INFLUENCE OF MORTAR BEDDING ON THE MECHANICAL BEHAVIOR OF HOLLOW CONCRETE MASONRY PRISMS UNDER AXIAL COMPRESSION

R.C. MATA[1]; H.L. LA ROVERE [2] and L.R. PRUDÊNCIO JR [3]

[1] Doctoral Student at the University of São Paulo – SET - EESC
São Carlos São Paulo Brazil
[2 and 3] Professors at the Federal University of Santa Catarina
Florianópolis Santa Catarina Brazil

SUMMARY

This work investigates both numerically and experimentally the influence of mortar bedding pattern on the compression behavior of hollow concrete masonry prisms. Linear elastic FE analyses were carried out, by modeling the prisms by solid elements, and by taking into account the tapering of the block face shells and webs. The experimental results indicated a loss of compressive strength, a more brittle failure mode, and earlier crack formation in the masonry prisms built with face shell bedding when comparing with prisms manufactured with full mortar bedding. Comparison between numerical and experimental stress-strain curves showed close agreement in the prism linear-elastic range.

INTRODUCTION

In the structural masonry construction process, the type of mortar bedding used when constructing walls can significantly affect productivity. However, the influence of mortar bedding type on the stress distribution, cracking, and failure mode of masonry walls has been investigated by researchers only to a small degree and neglected by structural engineers in structural masonry projects. Face shell bedding is coming to be used much more often because it enables faster execution. Moreover, it hinders water penetration in external walls, and therefore contributes to increasing construction durability.

Several authors have conducted experimental testing and finite element (FE) analyses on hollow concrete masonry prisms under axial compression (Drysdale *et al*, 1994). The influence of mortar bedding on prism behavior has been investigated experimentally by Maurenbrecher (1986); analytically by Hamid and Chucwunenye (1986), and Ganesan and Ramamurthy (1992); and both experimental and analytically by Shrive (1982). The experimental studies reported that prisms fabricated with only the face shell mortared exhibited vertical cracking through the webs at lower load levels than full-bedded prisms. Shrive (1982) explained that load transferred along the face shells produces nonuniform vertical stress along the blocks, and lateral stresses arise along the web, similar to flexural stress in deep beams. He pointed out that this effect is more pronounced for full capped prisms, which tends to reduce the strength of prisms. In the analytical studies, linear-elastic FE analyses on hollow prisms, modeled by solid elements, have been performed. The authors have found larger lateral stresses in the webs for face-shell bedded prisms, as compared to those found in full-bedded prisms. Hamid and Chucwunenye (1986), and Ganesan and

Ramamurthy (1992) utilized prisms that were 3-blocks high, but assumed a constant web and face shell thickness in the blocks. However, the tapering effect can significantly alter the stress distribution along the prism's height, as shown by Steil (2003) and by Shrive (1982). Shrive did model the block geometry accurately, but utilized a prism that was 2-blocks high in the FE analyses, which in general is not employed, due to platen restraint effects of the testing machine.

In order to investigate the influence of mortar bedding on the compression behavior of concrete masonry (built with mortar and units typically employed in Brazil) an analytical and experimental study of hollow masonry prisms and wallettes was conducted by the authors. This work describes the first part of the study, where only 3-block high and stack-bonded prisms, built with face shell and full mortar bedding, and using full capping, are analyzed. Prism compressive strength, elastic modulus and stress-strain curves were all measured experimentally. Linear elastic FE analyses were carried out, by modeling the prisms by a fine mesh of solid elements, and by taking into account the tapering of the block face shells and webs, in addition to the mortar bedding pattern.

EXPERIMENTAL PROGRAM

In the experimental program, the properties of the prism materials were first determined and then two series of prisms were constructed for the experimental compression tests, as described below.

HOLLOW BLOCK (UNITS)

The prisms were built using a type of hollow concrete block (commonly found on the market in Southern Brazil), which has a characteristic strength (f_{bk}) of 6 MPa. Criteria for the selection and acceptance of the blocks were defined in accordance with the requirements of the NBR 6136 Brazilian standard (1994). The block has standardized dimensions of 14x19x39 cm, with core dimensions as shown in Figure 1.

The physical characterization of the blocks described in Table 1 proceeded according to the NBR 6136 Brazilian standard (1994).

Table 1**.** Physical characteristics of the concrete blocks

Gross area	546.0 cm^2
Net area	339.1 cm^2
Ratio Net area / Gross area	62.11 %
Density	2.08 kg/dm^3
Absorption	6.11 %

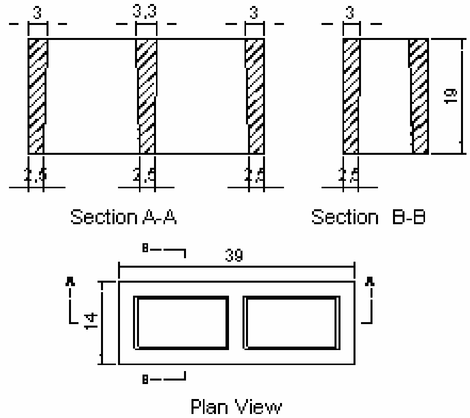

Figure 1. Geometry of concrete masonry units

BEDDING MORTAR

Cement-lime (cement, lime, and dry sand) bedding mortar was used for the units. The mortar's cement:lime:sand ratio was 1:1:5 (in volume) and its average compression strength was 5 MPa. The mortar mix proportions were based on the work of Steil (2003) and are commonly used for structural masonry construction in Brazil. Table 2 presents the mix proportions converted into mass and the average water/cement ratio.

The mortar was composed of CP II-F Portland cement, hydrated lime (CH-II), and a combination of natural sands, of which 90% was coarse sand and 10% was fine quartzose sand. The cement and lime had a specific gravity of 3.03 and 2.53 kg/dm³, respectively (determined according to the NBR NM23 Brazilian standard, 2001), and a bulk density equal to 1.10 and 0.73 kg/dm³, respectively (obtained following procedures from the NBR 7251 Brazilian standard, 1982).

Table 2. Mortar mix proportions

Type	Cement:lime:sand volume ratio	Cement:lime:sand mass ratio	Water/cement ratio
Cement-lime	1 : 1 : 5	1 : 0.66 : 6.05	1.46

PRISM CONSTRUCTION

For each type of mortar bedding, six 3-block high prism specimens were built and fully capped (see summary shown in Table 3). The bedding mortar was applied according to the types of mortar bedding under study, with a fixed joint thickness of 10±1 mm. During construction, prism level and plumb were verified (see Figure 2).

Table 3. Number of block and prism specimens

Type of mortar bedding	**Block**	**Prism**
Full	6	6
Face shell bedding	6	6
Total nb. of specimens	12	12

The compression tests were carried out when the prisms were 29 days-old. Six prisms and six units were tested under axial compression. The cylindrical mortar specimens were tested at 28 days.


Figure 2. Specimen construction (prisms and wallettes)

COMPRESSION TESTS AND INSTRUMENTATION

A LOSENHAULSENWERK 3000 kN hydraulic press test machine was employed in all tests, using a scale of 2000 kN. In this hydraulic press model, the load is applied in the direction opposite to gravity, i.e. the piston that applies the force is located at the base of the press.

Displacement transducers (in this case, linear variable differential transformers, or LDVTs) were employed for prism instrumentation. In order to obtain the strain from the block–mortar set deformation, two displacement transducers (LDVTs) were installed, as shown in Figure 3. With these data, it was thus possible to determine the elasticity modulus and the stress–strain curves for the prisms.

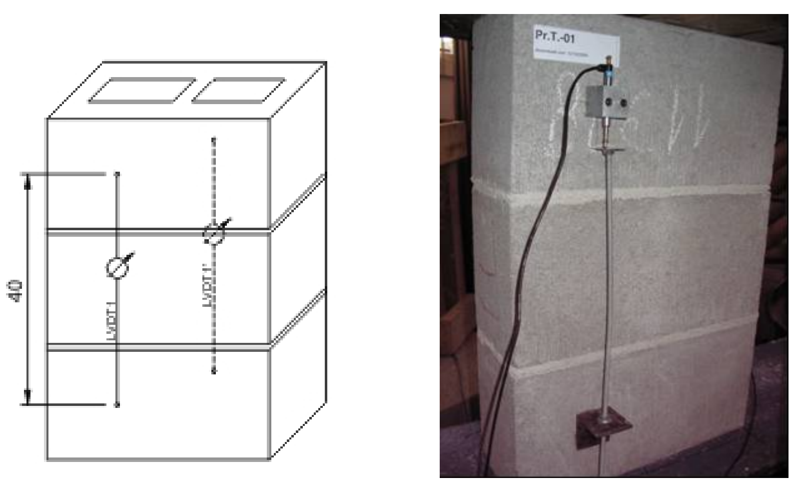

Figure 3. Position of LVDTs (LVDT1 on the front face of the prism and LVDT1' on the back face).

FINITE ELEMENT ANALYSIS

Numerical analysis of the prisms was carried out by means of the finite element method, using the SAP 2000 (2006) software. The goal of the analysis was to study the effect of face shell vs. full mortar bedding on the mechanical behavior of masonry prisms in the linear-elastic range.

Hexahedral isoparametric solid elements with eight nodes were used for discretization of the prisms. Data entry was accomplished by means of the graphical interface, making it possible to model any of the prism geometric peculiarities, including variation in the face shell and web thickness along the block's height (see Figure 4). The hollow block and mortar elasticity modulus values used in the numerical analysis were initially calculated in accordance with the NBR 6118 Brazilian standard (2003), using the experimental equation proposed by Mohamad (1998). Typical values of Poisson's ratio were assumed for the concrete block and mortar (see Table 4).

The load was applied at the base of the model (in the direction opposite to gravity, consistent with the test machine utilized) and it was calculated taking, as basis, 50% of the prism compressive strength, which was estimated using equation (1) proposed by Colville and Wolde-Tinsae (1990). Since this equation provides a conservative value for prism strength, it is expected that for this load level, the prism behaves linear-elastically. Table 5 shows estimated values for the block's net area and compressive strength.

$$f_m = 0.65 \times f_b \qquad (1)$$

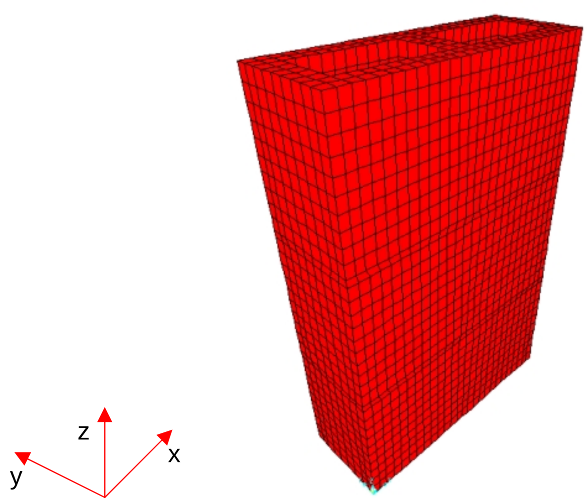

Figure 4. Prism FE model

Table 4. Properties of the hollow block and mortar

	Strength (MPa)	Modulus of elasticity (MPa)	Poisson (υ)
Hollow block	$f_{bk} = 11.5$	$E_b = 5600.\sqrt{f_{bk}}$ * **= 18.99 x 10³**	0.17
Mortar	$f_{ak} = 5.0$	$E_a = -18.9.f_{ak}^2 + 939.4.f_{ak}$ * **= 4.23 x 10³**	0.24

* where f_{bk} is expressed in MPa

Table 5. Characteristics of the hollow block

Gross area	546 cm²
Estimated compressive strength (gross area)	6.0 MPa
Net area*	285.9 cm²
Estimated compressive strength- f_b (net area)	11.5 MPa

* mean web thickness

By assuming that the mortar employed is of type N (5 MPa), equation (1) yields an estimated value of 7.48 MPa for the prism compressive strength (in the net area); hence the total compression load applied in the models was equivalent to a uniform stress of 3.74 MPa.

RESULTS

COMPRESSIVE STRENGTH

Most of the blocks tested presented a cone-shaped type failure, typical of confined specimens under compression. The average compressive strength in the net area was 16.31 MPa (see Table 6).

Table 6. Block compressive strength

Date of manufacture of hollow blocks: **23/05/2005**					
First test of compressive strength (full mortar bedding): **10/11/2005**					
Compressive Strength (MPa) (gross area)	Standard deviation (MPa)	Coefficient of variation (%)	Compressive Strength (MPa) (net area)*	Standard deviation (MPa)	Coefficient of variation (%)
8.21	0.92	11.22	**15.68**	1.76	11.22
Second test of compressive strength (face shell bedding): **24/11/2005**					
Compressive Strength (MPa) (gross area)	Standard deviation (MPa)	Coefficient of variation (%)	Compressive Strength (MPa) (net area)*	Standard deviation (MPa)	Coefficient of variation (%)
8.86	0.72	8.07	**16.93**	1.37	8.07

* Net area for mean web thickness

The tests enabled the determination of the prisms' compressive strength and corresponding strain, with both types of mortar bedding (see Table 7). In almost all of the cases, the type of failure that occurred was characterized by a vertical crack along the prism's smaller lateral faces. This type of failure was observed in the prisms with full mortar bedding and was even more notable for those with face shell bedding (see Figure 5).

Although the average compressive strength in the net area (which is considered equal to the mortar bedding area) of the prisms with face shell bedding was similar to that of the prisms with full mortar bedding, the mean failure load of the former was inferior to that of the latter by around 20%. The prism/unit ratio of the prisms with face shell bedding was 25% inferior to that of the prisms with full mortar bedding, due to fact that the former were composed of blocks presenting a slightly greater average compressive strength (see Table 7). It was also observed that the prisms with face shell bedding presented their first cracks for small loads, whereas those with full shell bedding presented visible cracks only when nearing failure.

The stress distribution along the prism webs obtained from the FE analyses is shown in Table 8 and Figure 6. It can be noted that much larger lateral stresses develop in the webs for face-shell bedded prisms, than for full-bedded prisms, confirming the experimental observations described above as well as the observations of other researchers (see Section 1).

Table 7. Prism compressive strength.

	Full mortar bedding		Face shell bedding	
Fail load (kN)	**383.41**		**309.83**	
	S.D. (kN)	27.65	S.D. (kN)	32.74
	C.O.V. (%)	7.21	C.O.V (%)	10.57
Compressive Strength (MPa) (gross area)	**7.02**		**5.67**	
	S.D. (MPa)	0.51	S.D. (MPa)	0.60
	C.O.V. (%)	7.21	C.O.V. (%)	10.57
Compressive Strength (MPa) (net area)	**13.41**		**13.24**	
	S.D. (MPa)	0.97	S.D. (MPa)	1.40
	C.O.V. (%)	7.21	C.O.V. (%)	10.57
Ratio Prism/Unit Ratio	**0.86**		**0.64**	
Mortar Compressive Strength (MPa)	**5.19**		**4.80**	
	S.D. (MPa)	0.50	S.D. (MPa)	0.42
	C.O.V. (%)	9.67	C.O.V. (%)	8.85

(a) (b)

Figure 5. Failure modes of masonry prisms: (a) Full mortar bedding; (b) Face shell bedding

Table 8. Summary of maximum tensile and compressive stresses in the middle block, for both face shell and full bedded prisms

Type of mortar bedding	Maximum Stress (MPa)		
	σ_x(tension)	σ_y(tension)	σ_z(compression)
Full	0.764	0.761	-4.793
Face shell bedding	1.123	3.762	-6.676
Ratio Face shell bedding/ Full	149.2%	501.2%	141.4%

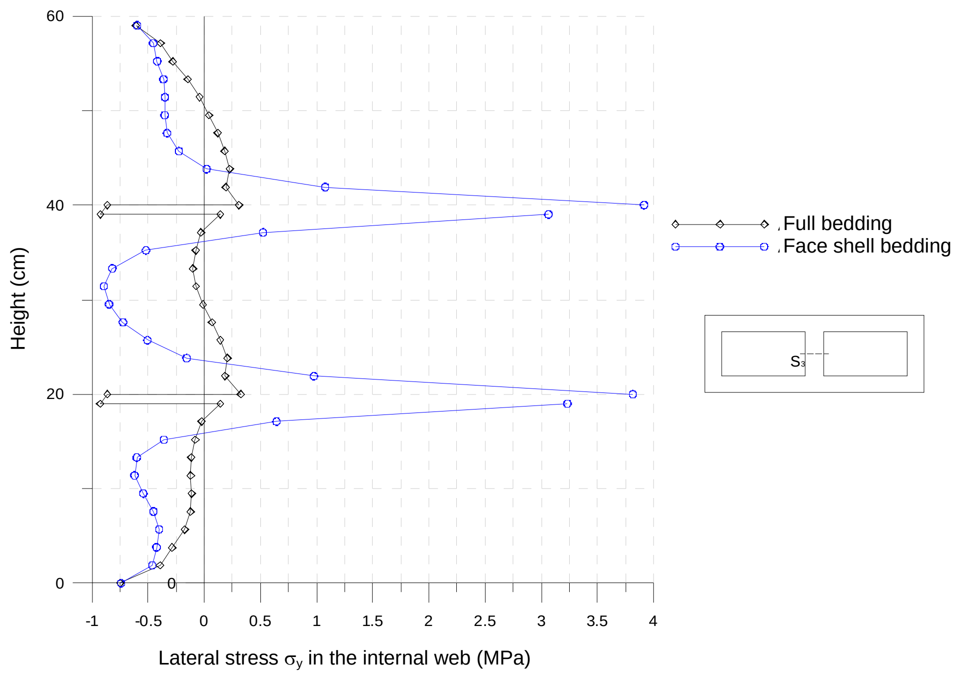

Figure 6. Comparison between stress distribution σ_y along the prism central web obtained from the FE analyses of full bedded and face shell bedded prisms

COMPARISON BETWEEN NUMERICAL AND EXPERIMENTAL RESULTS

The secant elastic modulus of the prisms was determined by following the procedure described in ACI530/ASCE/TMS402 (1996), from a straight line connecting the points corresponding respectively to 5% and 33% of the maximum compressive stress on the stress–strain experimental curves. These curves were plotted using the following two parameters: the stress in the net area (the mortar bedding area) and the strain. The latter is equal to the average of the displacements (measured by LVDT1 and LVDT1') over the length of the LVDT rod (see Figure 3). Table 9 shows mean values obtained for prism modulus of elasticity.

To determine the modulus of elasticity from the numerical results, stress vs. strain curves were plotted, where strain is calculated by dividing the relative displacements at the points corresponding to the top and bottom of the LVDT rod by the length of the rod (see Figure 3), as done to obtain the experimental stress-strain curves. As previously mentioned, in the finite

element analysis a stress of 3.74 MPa (in the net area) was applied. The numerical and experimental results for prism modulus of elasticity are compared in Table 10.

Table 9. Results for modulus of elasticity (net area)

Mortar bedding type	Modulus of elasticity (MPa)	$\frac{E}{f_m}$
Full bedding	$17.17\text{x}10^3$	1280
Face shell bedding	$16.74\text{x}10^3$	1264

Table 10. Results for modulus of elasticity (net area)

Mortar bedding type	Experimental modulus of elasticity (MPa)	Numerical modulus of elasticity (MPa)
Full bedding	$17.17\text{x}10^3$	$17.81\text{x}10^3$
Face shell bedding	$16.74\text{x}10^3$	$15.29\text{x}10^3$

The elasticity modulus value obtained numerically for the prisms with full mortar bedding is 3.6% greater than that determined experimentally, whereas for the prisms with face shell mortar bedding, the numerical value is 9.5% lower than the experimental one.

Figure 7 displays the lines plotted to determine the numerical and experimental values for the modulus of elasticity of: (a) prisms with full mortar bedding, and (b) prisms with face shell bedding. On the one hand, it can be seen that in the case of the prisms with full mortar bedding, the plotted line obtained through finite element analysis is a good fit for a mean experimental curve in the linear-elastic range. On the other hand, for the prisms with face shell bedding, the finite element model is slightly different than the experimental one.

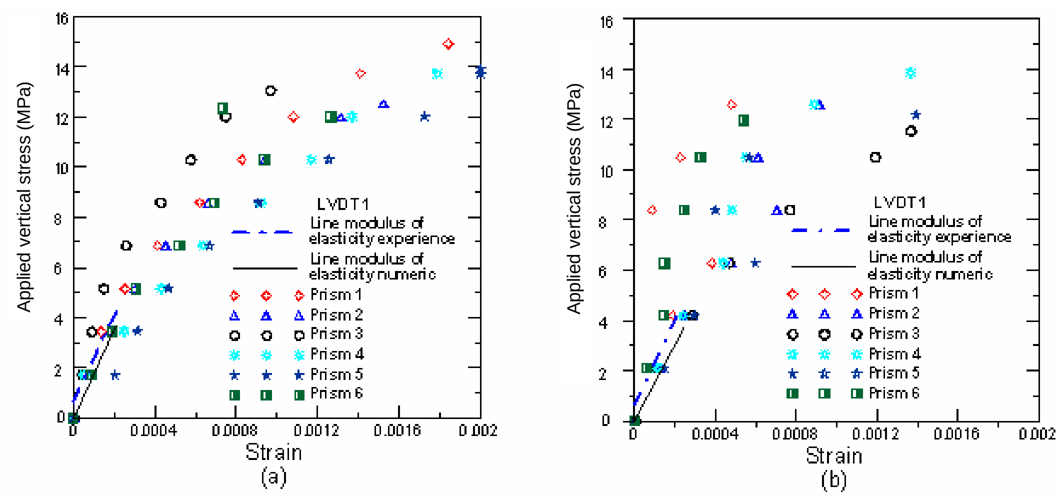

Figure 7. Lines plotted for modulus of elasticity (experimental and numerical): (a) Full mortar bedding; (b) Face shell bedding

CONCLUSION

In compression tests with both types of mortar bedding, all of the experiments indicated that the failure loads for the prisms with face shell bedding were inferior to those of the prisms with full mortar bedding. Similarly, the prism/unit ratio of specimens with face shell bedding

was shown to be inferior to that of the full mortar bedding specimens. Another important finding is that, in a majority of cases, the behavior of the face shell bedding prisms during failure was characterized by greater strains and loss of integrity in specimens.

Numerical and experimental results were compared by means of stress–strain and elasticity modulus diagrams. In general, there was a good agreement between numerical and experimental results within the bounds of the elastic regime, especially for the prisms with full mortar bedding.

From the results of the experimental analyses, it can be concluded that the type of mortar bedding considerably influences the mechanical behavior of masonry under axial compression. Prisms built with face shell bedding were characterized by smaller prism/unit ratios and a more brittle failure mode, as well as earlier crack formation at the transverse webs, when comparing with prisms manufactured with full mortar bedding.

Thus, although face shell mortar bedding presents certain advantages with respect to reducing execution time and avoiding water penetration, based on the results presented here, care should be taken in the design of structural walls, since cracking could occur at service load levels. Similar results were found for wallettes built with face shell bedding (Mata, 2006). Other effects like capping are currently being investigated, both numerically and experimentally.

REFERENCES

American Concrete Institute; American Society of Civil Engineeres. "Building Code Requirements for Masonry Structures". *The Masonry Society American*. ACI530/ASCE 5/TMS 402, Detroit, 1996.

Association Brazilian of Standards (NBR). "Bloco vazado de concreto simples para alvenaria estrutural: especificação". NBR 6136**.** Rio de Janeiro, 1994.

Association Brazilian of Standards (NBR). "Projeto de estruturas de concreto armado"**.** NBR 6118. Rio de Janeiro, 2003.

Association Brazilian of Standards (NBR). "Agregado em estado solto - Determinação da massa unitária". NBR 7251. Rio de Janeiro, 1984.

Association Brazilian of Standards (NBR). "Cimento portland e outros materiais em pó: determinação da massa específica". NBR NM 23. Rio de Janeiro, 2001.

Colville, J., Wolde-Tinsae, A., "Compressive strength of hollow concrete masonry". *Proceedings of the Fifth North American Masonry Conference.* Vol. II, June 1990, pp. 663 – 672.

Drysdale, R.G., Hamid, A.A., Baker, L.R., "Masonry Structures - Behavior and Design". *Ed. Prentice Hall,* Englewood Cliffs, New Jersey, 1994.

Ganesan, T.P., Ramamurthy, K., "Behavior of concrete hollow-block masonry prisms under axial compression". *Journal of Structural Engineering*, ASCE, Vol. 118, No. 7, July 1992, pp. 1751-1769.

Hamid, A., Chucwunenye, A., "The compression behavior of concrete masonry prisms". *Journal of the Structural Division*, Proceedings of the ASCE, Vol. 112, No. 3, March 1986, pp. 605-614.

Mata, R. C., "Influence of mortar bedding on the compressive strength of concrete masonry wallettes and prisms". 2006. 180p. Msc. Dissertation (Civil Engineering Program - PPGEC) – Federal University of Santa Catarina, Florianópolis (*in Portuguese*).

Maurenbrecher, A.H.P., "Compressive strength of hollow concrete blockwork". *Proceedings of the Fourth Canadian Masonry Symposium*, June 1986, pp. 997-1009.

Mohamad, G., "Mechanical behavior at failure of concrete masonry prisms"**.** 1998. 178p. Msc. Dissertation (Civil Engineering Program - PPGEC) – Federal University of Santa Catarina, Florianópolis (*in Portuguese*).

SAP2000 – Computers and Structures, Inc. Version 10.0, 2006.

Shrive, N.B., "The failure mechanism of face shell bedded ungrouted and unreinforced masonry". *International Journal of Masonry Construction*, Vol. 2, No. 3, 1982, pp.115-128.

Steil, R. O. "The effect of block geometry and mortar type in the compression behavior of ungrouted concrete masonry prisms". 2003. Msc. Dissertation (Civil Engineering Program-PPGEC) – Federal University of Santa Catarina, Florianópolis (*in Portuguese*).